

Pitch angle variation and turbulence profiles in ASDEX-Upgrade

N P Basse^{1,2}, G D Conway³ and M Endler³

30th of July 2001

¹ Association EURATOM - Risø National Laboratory, DK-4000 Roskilde, Denmark

² H.C. Ørsted Laboratory, Niels Bohr Institute for Astronomy, Physics and Geophysics, DK-2100 Copenhagen, Denmark

³ Association EURATOM - Max-Planck-Institut für Plasmaphysik, D-85748 Garching, Germany

1 Introduction

An initial memo was prepared investigating the feasibility of three lines-of-sight (LOS) for a CO₂ laser based scattering system on ASDEX-Upgrade (AUG) [1]. One vertical and two tilted LOS were considered; it was concluded that both of the tilted LOS would be suitable for implementation. Four operational scenarios were treated, and the total pitch angle variation was between 9 and 19 degrees. An objection raised by H Bindslev in response to the memo was that it is the pitch angle θ_p projected onto the plane perpendicular to the LOS that is relevant, and not the angle

$$\theta_p^z = \arctan\left(\frac{B_z}{B_\varphi}\right) \quad (1)$$

used in the memo. The purpose of this report is two-fold:

1. Derive the full expression for the pitch angle for tilted LOS (section 2)
2. Having obtained the pitch angle variation, calculate scattered power versus selected plasma position (section 3)

2 Pitch angle derivation

We will treat LOS L1, AUG shot 14034, an internal transport barrier (ITB) shot, case 2 in [1]. Here, $(S_R, S_z) = (R_2 - R_1, z_2 - z_1) = (1.11-2.24 \text{ m}, -0.59-0.48 \text{ m})$ are the LOS coordinates. The magnetic field components along the LOS are plotted versus the normalised minor radius ρ in figure 1. B_R is the dotted line, B_z the dashed line and B_φ is represented by the solid line.

The first geometrical quantity to be determined is the angle of the LOS with respect to horizontal. This angle is given by

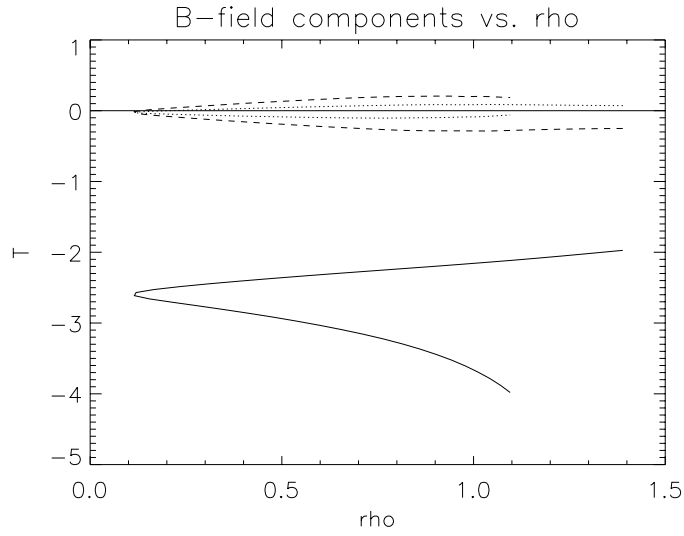


Figure 1: Magnetic field components, case 2. B_R is the dotted line, B_z the dashed line and B_φ is represented by the solid line.

$$\theta_{\text{LOS}} = \arctan\left(\frac{z_2 - z_1}{R_2 - R_1}\right), \quad (2)$$

which is 43.4 degrees for our example. The next task is to project the B_R and B_z components onto the plane perpendicular to the LOS. The resulting component is

$$B_{Rz}^{\text{proj}} = B_z \cos \theta_{\text{LOS}} - B_R \sin \theta_{\text{LOS}} \quad (3)$$

Finally, since B_φ lies in the orthogonal LOS plane, it should not be modified. Collecting the results, the pitch angle in the plane perpendicular to the LOS is

$$\theta_p = \arctan\left(\frac{B_{Rz}^{\text{proj}}}{B_\varphi}\right) = \arctan\left(\frac{B_z \cos \theta_{\text{LOS}} - B_R \sin \theta_{\text{LOS}}}{B_\varphi}\right) \quad (4)$$

The two limits for horizontal and vertical LOS are

$$\begin{aligned} \theta_p(\theta_{\text{LOS}} = 0 \text{ degrees}) &= \arctan\left(\frac{B_z}{B_\varphi}\right) = \theta_p^z \\ \theta_p(\theta_{\text{LOS}} = 90 \text{ degrees}) &= \arctan\left(\frac{-B_R}{B_\varphi}\right), \end{aligned} \quad (5)$$

where θ_{LOS} is 0/90 degrees for a horizontal/vertical LOS, respectively.

Since we have the components of both \vec{B} and \vec{S} , we can calculate the pitch angle versus ρ . To compare the method used in [1] and derived above, we show θ_p (solid line) and θ_p^z (dotted line) versus ρ in figure 2.

The conclusion is that the angles are very similar, and therefore the conclusions drawn in [1] remain valid, at least for the L1 LOS.

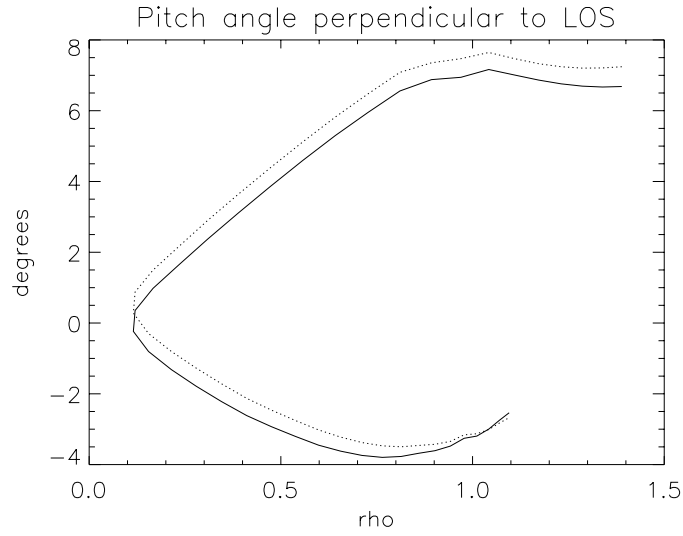


Figure 2: Pitch angles compared. Solid line is θ_p , dotted line θ_z . The +7.5 degree angle is low field side (LFS), -3.5 degrees high field side (HFS).

3 Turbulence profiles

The signal observed by the scattering diagnostic is not simply density fluctuations, but density fluctuations squared (δn_e^2) multiplied by an instrumental function; the product is integrated along the LOS [2]. NOTE: The fluctuation profiles and scattered power below are always in arbitrary units; no absolute calibration has been done. For the calculations we assume a relative fluctuation profile having shape

$$\delta n_e/n_e = b + c\rho^p, \quad (6)$$

where b , c and p are fit parameters. Below we use $c/b = 197$ and $p = 7.2$, the W7-AS L-mode profile [3]. Further, since we have no density profile measurements available for the design study, we take the normalised density to be

$$n/n_0 = 0.1 + 0.9\sqrt{(1 - \rho^2)} \quad (7)$$

Once we have this information and the pitch angle variation, the only remaining input is the measurement volume waist w and the wavenumber selected k_\perp . Thereafter we are able to calculate the total scattered power observed by the diagnostic as a function of the spatial position determined by varying the wavenumber angle α . Good localisation means that the product wk_\perp has to be large:

$$\frac{2}{wk_\perp} \times \frac{180}{\pi} \ll |\theta_p(\text{LFS}) - \theta_p(\text{HFS})| \quad (8)$$

In figure 3 we show scattered power versus α for a fixed k_\perp of 20 cm^{-1} . The left-hand plot is for a waist w of 1 cm (narrow volume), right-hand plot for a waist of 3 cm (wide volume). It is obvious that the variation of scattered power for a narrow volume is small,

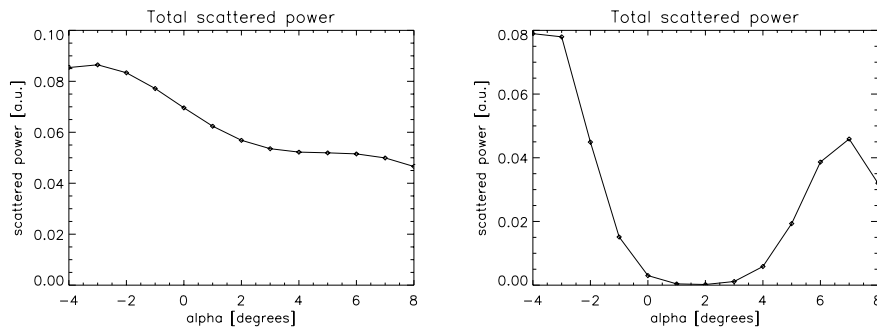


Figure 3: Modelled scattered power integrated along LOS L1 versus diagnostic angle α . Left: $w = 1$ cm, $k_{\perp} = 20$ cm $^{-1}$, right: $w = 3$ cm, $k_{\perp} = 20$ cm $^{-1}$.

but pronounced for the wide volume. So a volume waist of about 3 cm will be sufficient to guarantee excellent localisation, even at this comparatively small wavenumber.

For actual measurements the procedure will be inverse of the one sketched above: Measurements will provide data as that shown in figure 3; supplying a measured density profile the remaining unknown is the relative fluctuation profile which is extracted by assuming a profile shape and making a least-squares-fit to the measurements [3].

4 Conclusions

We have shown that good spatial localisation of density fluctuations can be achieved using a double-pass wide volume diagnostic having a tilted LOS. The total pitch angle variation for LOS L1 ranges between 9 and 19 degrees for the four cases presented in [1], while the wavenumber resolution (left-hand side of equation (8)) for a beam diameter $2w$ of 6 cm and wavenumber of 20 cm $^{-1}$ is 1.9 degrees. This means that localisation is possible for all case studies.

Standard reflectors of infrared light (as opposed to retroreflectors) mounted on the inner wall of AUG are quite insensitive to vibrations [4]. We suggest as the next step in the design process that it is determined where mirrors can be placed above and below the heat shield. The diameter of the mirrors for a 6 cm volume diameter should be roughly 12 cm (two times volume diameter) to minimise edge diffraction effects.

References

- [1] Conway G D, Memo 24th of July 2001
- [2] Truc A et al., Rev. Sci. Instrum. **63** (1992) 3716
 Devynck P et al., Plasma Phys. Control. Fusion **35** (1993) 63
 Antar G et al., Phys. Plasmas **8** (2001) 186
- [3] Basse N P et al., Proc. of the Int. Conf. on Phenomena in Ionized Gases, July 17-22 Nagoya, Japan **4** (2001) 335
- [4] Gehre O, private communication (2001)